Intelligent Automation & Soft Computing

Tech Science Press

DOI: 10.32604/iasc.2024.058416

ARTICLE

Enhanced Diagnostic Precision: Deep Learning for Tumors Lesion Classification in Dermatology

Rafid Sagban[1,2,*], Haydar Abdulameer Marhoon[3,4] and Saadaldeen Rashid Ahmed[5,6,*]

[1]Engineering Technical College, Al-Ayen University, Thi-Qar, 64001, Iraq

[2]Information Technology College, University of Babylon, Hilla, 51001, Iraq

[3]Information and Communication Technology Research Group, Scientific Research Center, Al-Ayen University, Thi-Qar, 64001, Iraq

[4]College of Computer Sciences and Information Technology, University of Kerbala, Karbala, 56001, Iraq

[5]Artificial Intelligence Engineering Department, College of Engineering, Al-Ayen University, Thi-Qar, 64001, Iraq

[6]Computer Science, Bayan University, Erbil, 44001, Iraq

*Corresponding Authors: Rafid Sagban. Email: rsagban@alayen.edu.iq; Saadaldeen Rashid Ahmed. Email: saadaldeen.ahmed@alayen.edu.iq

Received: 11 September 2024 Accepted: 10 December 2024 Published: 30 December 2024

ABSTRACT

Skin cancer is a highly frequent kind of cancer. Early identification of a phenomenon significantly improves outcomes and mitigates the risk of fatalities. Melanoma, basal, and squamous cell carcinomas are well-recognized cutaneous malignancies. Malignant We can differentiate Melanoma from non-pigmented carcinomas like basal and squamous cell carcinoma. The research on developing automated skin cancer detection systems has primarily focused on pigmented malignant type melanoma. The limited availability of datasets with a wide range of lesion categories has hindered in-depth exploration of non-pigmented malignant skin lesions. The present study investigates the feasibility of automated methods for detecting pigmented skin lesions with potential malignancy. To diagnose skin lesions, medical professionals employ a two-step approach. Before detecting malignant types with other deep learning (DL) models, a preliminary step involves using a DL model to identify the skin lesions as either pigmented or non-pigmented. The performance assessments accurately assessed four distinct DL models: Long short-term memory (LSTM), Visual Geometry Group (VGG19), Residual Blocks (ResNet50), and AlexNet. The LSTM model exhibited higher classification accuracy compared to the other models used. The accuracy of LSTM for pigmented and non-pigmented, pigmented tumours and benign classes, and melanomas and pigmented nevus classes was 0.9491, 0.9531, and 0.949, respectively. Automated computerized skin cancer detection promises to enhance diagnostic efficiency and precision significantly.

KEYWORDS

Pigmented lesions; deep learning models; skin cancer; automated diagnosis; basal cell carcinoma

1 Introduction

The rising incidence of skin cancer, particularly melanoma, underscores the urgent need for enhanced diagnostic techniques. While current practices like skin biopsies remain the gold standard for diagnosis, they are time-consuming and invasive. Automated deep learning (DL) systems promise to make diagnoses more accurate, especially when it comes to telling the difference between skin lesions that are coloured and those that are not. This study examines how well DL models like LSTM, VGG19, ResNet50, and AlexNet can sort different skin lesions, help find them earlier, and give dermatologists better diagnostic tools.

One of the most deadly skin cancers is melanoma. Globally, cutaneous malignancies account for 75% of mortality due to melanoma. Melanoma can inhibit the formation of melanin due to its impact on the cells responsible for melanin synthesis [1]. Given these circumstances, the early identification of melanoma assumes significant importance in the battle against cancer-related death, as shown in Fig. 1.

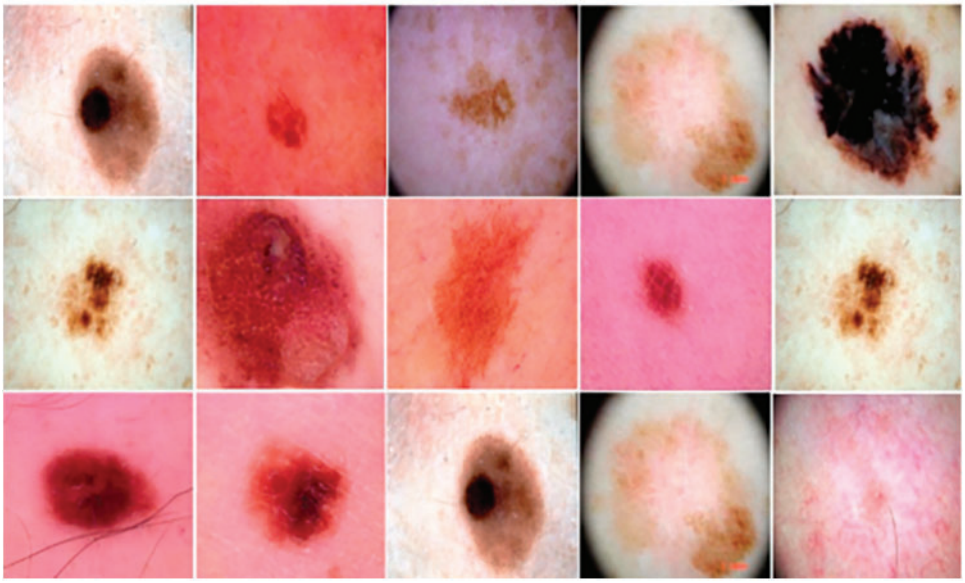

Figure 1: Some samples from the dataset

We can broadly classify skin lesions into two primary categories: pigmented and non-pigmented. Both melanoma and pigmented nevi are instances of pigmented lesions. Similarly, non-pigmented lesions encompass vascular issues, basal cell cancer, dermatofibroma, and actinic keratosis, the initial manifestation of squamous cell carcinoma, commonly referred to as Bowen's disease. We can classify pigmented and non-pigmented lesions as benign or malignant. Melanoma, basal cell carcinoma, and actinic keratosis are all examples of skin conditions that are malignant, which means they can cause cancer.

Scanning is a commonly used non-invasive imaging method that studies the morphology of skin lesions. Fig. 1, the provided dermoscopy images, shows the melanoma skin lesion. Dermatoscopy is a useful way to find melanoma early on because pigmented lesions can sometimes show signs of not being pigmented. The people who discussed dermoscopy agreed to use a two-step diagnostic method to group skin lesion pigmentation seen with dermoscopy [2,3]. The implementation of this measure aimed to standardise dermoscopic nomenclature. After explaining the difference between pigmented

and non-pigmented lesions, the next step in this process is to explain the difference between benign and malignant lesions.

Unfortunately, this instrument's complex and time-consuming framework occasionally compromises its efficacy, as does its limited ability to consistently distinguish between inter- and intra-features. Furthermore, we can employ computational methods to expand the use of dermoscopy [4]. An arduous implementation of this idea involves using computer methods to categorise melanomas using artificial segmentation, considering factors such as size, colour, form, and texture (Fig. 2).

The primary outcomes derived from this research are:

- Commodifying non-pigmented skin lesions augments dermatologists' two-step dermoscopic procedure [3].
- In contrast to previous research that used clinical imaging to categorize malignant, non-pigmented skin lesions, the present study utilizes dermoscopy pictures [5]. The presence of photographic variability can influence the clinical imaging process.
- We used a collection of 7285 dermoscopy pictures to more accurately classify pigmented skin lesions that are not pigmented. This collection is substantially larger than the 167 [6] or 107 [7] photos used in earlier study projects.
- To broaden the classification of non-pigmented skin lesions, we have included vascular lesions in addition to the dermatofibroma categories. In the study above, we classified these two common forms of benign, non-pigmented skin lesions in clinical practice using only fourteen out of six hundred fifty photographs [7]. However, binary non-pigmented skin lesions classification has overlooked these groups in studies [6] and [8].

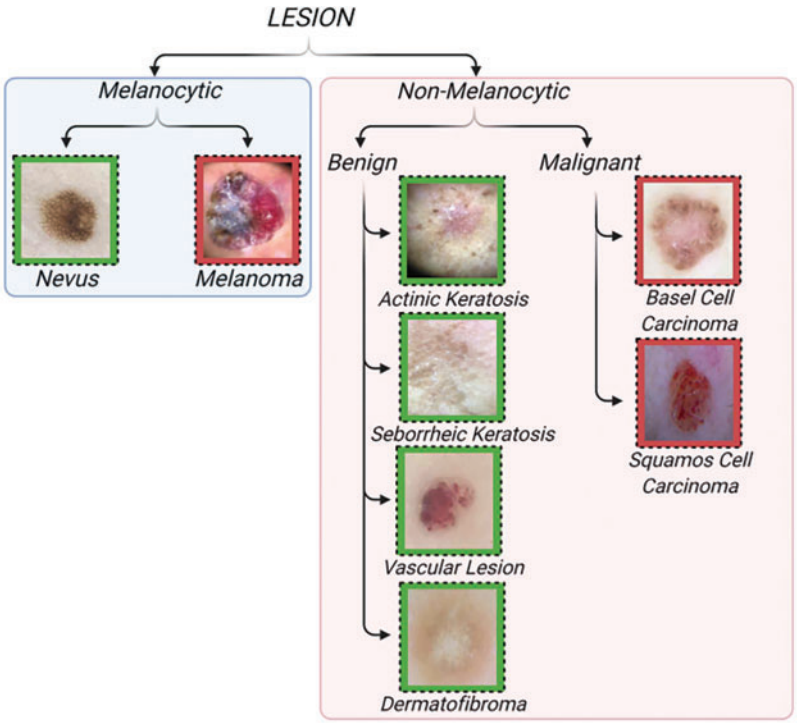

Figure 2: Classification of skin lesions [3]

The following section outlines the organizational structure of the paper: Preceding this, one may encounter pertinent scholarly material about machine-learning approaches for classifying skin lesions. The next part explains the research techniques employed in this study and the database used for data collection and analysis. Finally, we evaluated and discussed the efficacy of the DL architecture.

2 Related Works

Melanoma identification in dermoscopic images employs two primary strategies: deep learning (DL) and classical methods. Initial efforts relying on manually designed features exhibited limited effectiveness. For instance, Reference [9] introduced the California STEM Learning Network (CSLNet), a specialised deep convolutional neural network (CNN) trained on the ISIC-19 dataset using end-to-end learning that achieves superior performance across various metrics without relying on handcrafted features. Concurrently, Reference [10] proposed an algorithm to optimise wavelet networks by enhancing feature selection to improve melanoma detection effectiveness. However, both approaches struggled to distinguish melanoma subtypes and differentiate visual similarities between melanoma and non-melanoma images [1].

To address these challenges [11], we combined neural networks with genetic algorithms, emphasising segmentation methodologies. Border detection techniques extracted clinical features like border irregularity and asymmetry. However, this method faced issues resolving indistinct boundaries in unclear lesions, complicating melanoma diagnosis [12].

Han et al. [13] compiled over 20,000 macroscopic images spanning 12 disease classes and utilised a fine-tuned ResNet-152 model [14] to freeze early layers for feature extraction from manually cropped images. Similarly, Ma et al. [15] demonstrated using pre-trained ConvNets for classifying non-dermoscopic skin images through feature extraction. In addition, Reference [16] used a multi-stage, multi-scale method and a softmax classifier to sort melanoma lesions by pixel.

The utility of CNNs in melanoma detection lies in their ability to effectively perform identification, classification, and segmentation tasks. For example, Reference [17] developed a hybrid model integrating a CNN with sparse coding and a support vector machine (SVM) algorithm. A non-supervised CNN model based on AlexNet was also proposed by [7], aiming to extract features specific to melanoma.

A deep learning method for separating melanoma lesions first described by [4] used a fully convolutional network (FCN) with 19 layers. The convolution operator improved the accuracy, but FCNs had problems like being less flexible because they had fewer parameters, were less efficient than Maxpool operators, and took longer to train. We validated this approach using ISIC 2016 and PH datasets.

Expanding into more medical imaging, Reference [18] created HGANet, a CNN for automatically finding problems in the digestive tract using Kvasir datasets. This demonstrates the effectiveness of Deep Learning in medical image analysis. The study [19] reviewed smartphone applications for skin disease diagnosis using Convolutional Neural Networks (CNNs). It employs digital photographs and dermoscopy images as datasets. CNNs enhance classification accuracy without user intervention. Results show that while many apps assist in skin cancer detection, few offer direct computational analysis with varying performance metrics.

Deep learning systems (DLS) [20] identify skin disorders based on clinical cases (skin pictures and medical history). The DLS recognises 26 skin disorders—80% of primary-care skin problems. We

created and tested the DLS using de-identified cases from 17 teledermatology clinics that were spread out over time.

The SPL analysis method is based on a deep convolutional neural network and works with wide-field photos [21]. It was tested on a dermatology dataset containing 38,283 images which included 133 patient images used in the ISBI 2016 dataset, which has 900 dermoscopy images [22].

The PH^2 dataset, which has 200 images split into three groups, to make sure that their methods worked.Different pre-trained state-of-the-art architectures (DenseNet 201, ResNet 152, Inception v3, InceptionResNet v2) were used by applied on applied 10,135 dermoscopy skin images in total (HAM10000: 10015, PH2: 120). This study utilises the 2019 ISIC Challenge dataset (Fig. 3) [8], encompassing 30,169 dermoscopy images across seven categories, facilitating DL frameworks for distinguishing pigmented and non-pigmented tumour lesions (Table 1).

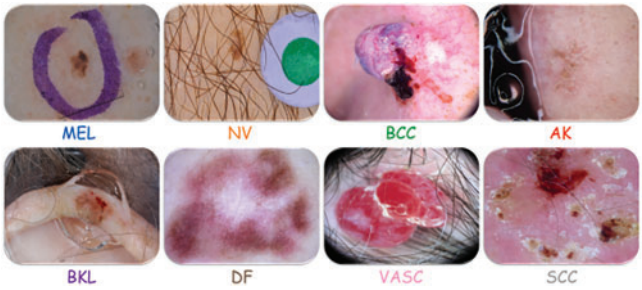

Figure 3: Skin lesions of ISIC 2019

Table 1: Recent studies (2023–2024)

Study	Model	Dataset	Method	Accuracy	Remarks
[23]	CNN	HAM10000	Adam optimiser, data augmentation, early stopping, model checkpoint	97.858%	Effective for identifying melanoma and basal cell carcinoma.
[24]	CNN	ISIC	Data augmentation	87.64%	Improves diagnosis over traditional methods
[25]	DTL + ML	HAM10000, DAYISET 1	XGBoost with Lasso regression, ROC curves, confusion matrix	AUC: 1.0 (train), 0.708 (validation)	Enhances BCC and AK detection.
[26]	Mobile Net-V2	1559 images	Transfer learning, fine-tuning, Grad-CAM for explainability	~90%	Strong performance; struggles with minority classes.
[27]	CNN	57,822 images	Deep learning, multi-staining protocols	94.6%	Reliable across staining protocols.

(Continued)

Table 1 (continued)

Study	Model	Dataset	Method	Accuracy	Remarks
[28]	ResNet50, ViT	ImageNet, skin cancer	Transfer learning, CAM-based explainability	ResNet50: 88.8%	Balances accuracy and complexity; requires dermatologist input.
[29]	Ensemble	ISIC 2018	Ensemble learning using multiple deep models	93.18%	Outperforms existing skin lesion classifiers.
[30]	Ensemble	1659 images	U-Net for segmentation, hyperspectral imaging, XGBoost	93.51%	Excels in PsO classification; efficient but slower inference.
[31]	STFL	HAM10000	Semi-supervised learning, dynamic threshold adjustment	85.50%	Performs well with limited labelled data.
[32]	DC-AC	SIIM-ISIC 2020	Transfer learning, data augmentation	AUROC: 0.9787	High efficiency with fewer parameters.

3 Methodology

The main goal of developing and testing four different deep learning (DL) models, namely Long Short-Term Memory (LSTM), VGG19, ResNet50, and AlexNet, is to distinguish between cancerous skin lesions and those that are not. The process involves three main phases: data preprocessing and augmentation, model development, and model evaluation.

3.1 Data Preprocessing and Augmentation

This work uses a collection of pictures of melanocytic and non-melanocytic skin lesions. The pictures came from the 2019 ISIC challenge collection, which is open to the public and has 25,331 pictures of different skin diseases. Table 2 illustrates the initial uneven distribution of the dataset's pictures among the various groups.

Table 2: Initial classification of melanoma and non-melanoma cells

Skin lesion	Training set	Testing set	Total
Melanoma cells	4525	862	5387
Non-melanoma	20,729	4053	15,267
Total	25,254	4915	30,169

Different augmentation approaches [33–35] used data augmentation methods like image rotation, flipping, zooming, and scaling to fix the imbalance because they were fast on the computer. This process increased the dataset size and ensured that each category contained a more even distribution of images, as shown in Table 3. The augmentation process improved the model's ability to generalise across different lesion types by exposing it to a wider range of variations in the training set.

Table 3: Balanced data after augmentation

Skin lesion	Training set	Testing set	Total
Melanoma cells	19,867	1418	20,729
Non-melanoma	20,729	4053	24,782
Total	40,596	5471	46,067

Data preprocessing for this study involves resizing all images to a uniform dimension of 224 × 224 pixels to ensure consistency across the dataset and normalising pixel values to a range of [0, 1] by dividing by 255, which improves model convergence during training. We apply data augmentation techniques to enhance the diversity of the dataset. These include random rotations within a range of −30 to +30 degrees to simulate different orientations, horizontal and vertical flipping to create mirror images, zooming from 0.8 to 1.2 to simulate different camera distances, and shearing transformations to introduce perspective changes. Additionally, brightness adjustments between 0.8 and 1.2 account for lighting variations. At the same time, colour jittering modifies hues and saturations to simulate different lighting conditions. We also employ random cropping, which shifts the image width and height by 10% to focus on different parts of the lesions. We implement these techniques using Keras' ImageDataGenerator, forming an augmentation pipeline that applies these transformations in real-time during model training through batch generation and the flow method.

3.2 Model Development

We developed four DL models to classify skin lesions—LSTM, VGG19, ResNet50, and AlexNet. We trained each model to identify both pigmented and non-pigmented skin lesions. The pigmented category includes melanoma and pigmented nevus. In this group are basal cell carcinoma (BCC), actinic keratosis (AK), benign keratosis (BKL), dermatofibroma (DF), and vascular lesions (VASC). However, they are not coloured.

We employed the Keras deep learning framework for model implementation. The need to balance accuracy and computational efficiency drove the choice of architecture. We used already trained models (VGG19, ResNet50, and AlexNet) to make transfer learning easier. The ISIC dataset was used to fine-tune the models. We incorporated LSTM to capture temporal dependencies in lesion features, enhancing the model's ability to classify images with subtle variations. The Machine Learning Models Training & Testing Framework for the 2019 ISIC Challenge Dataset is depicted in Fig. 4.

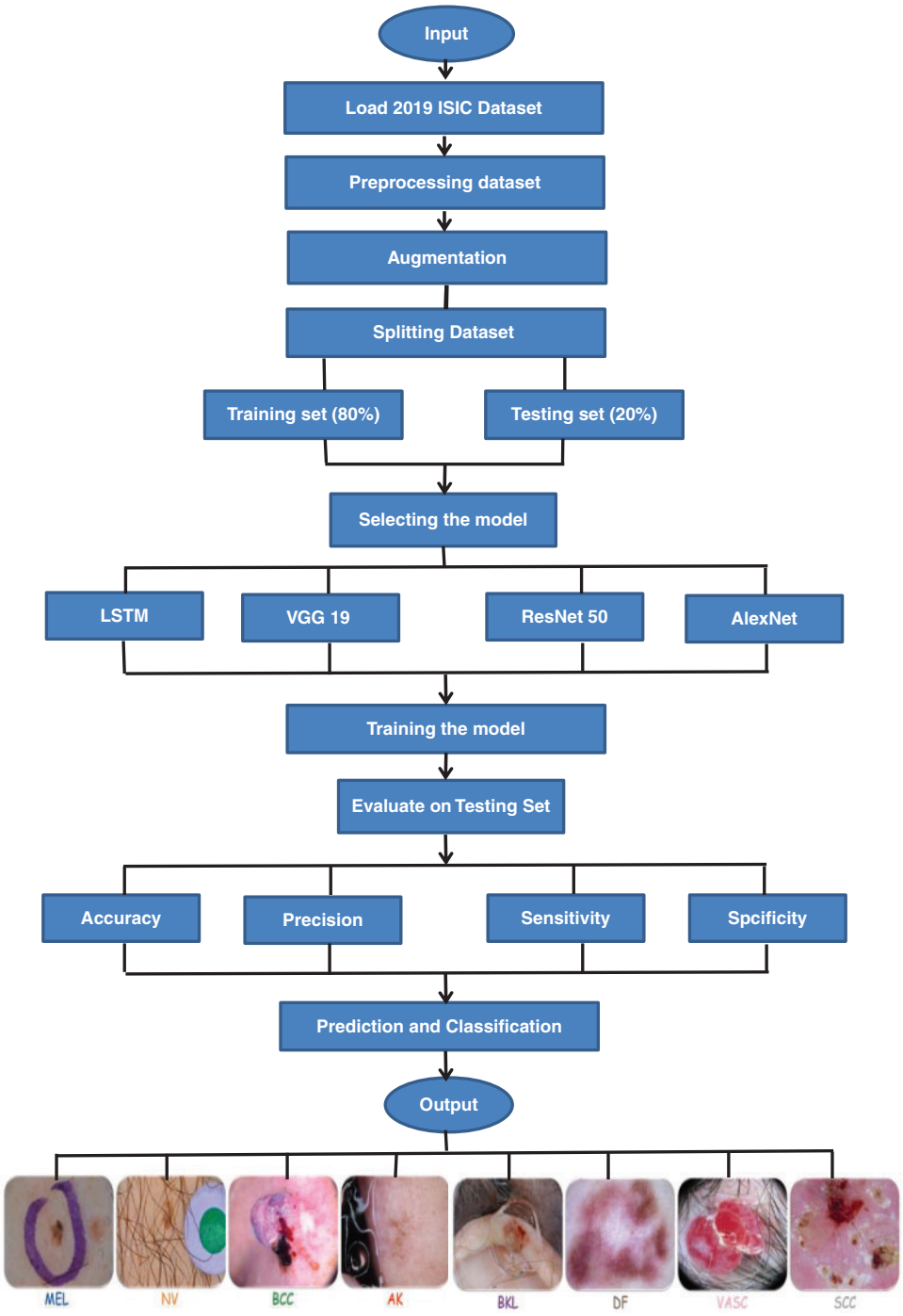

Figure 4: The framework of this study

Additional augmentation techniques were applied to further balance the dataset between melanoma. They pigmented nevus, as shown in Tables 4 and 5.

Table 4: Classification of melanoma and pigmented nevus

Skin lesion	Training set	Testing set	Total
Melanoma	4525	862	5387
Pigmented nevus	9581	2078	11,659
Total	14,106	2940	17,046

Table 5: Balanced data after augmentation (melanoma *vs*. pigmented nevus)

Skin lesion	Training set	Testing set	Total
Melanoma	10,668	862	11,530
Pigmented nevus	9581	2078	11,659
Total	20,249	2940	23,189

DL models are used to classify benign and non-pigmented malignant tissues accurately. Non-pigmented benign tumours include benign keratosis, dermato-fibroma, and vascular lesions. Conversely, basal cell carcinoma and actinic keratosis (commonly known as Bowen's disease) are two instances of non-pigmented malignant tumours. Table 6 displays the number of photographs allocated to each category.

Table 6: Non-pigmented tumour and benign classes

Skin lesion	Training set	Testing set	Total
Tumor	1858	347	2205
Benign	4782	964	5746
Total	6640	1311	7951

3.3 Hyperparameters and Training Configuration

The hyperparameters utilized in the training process are summarized in Table 7. These values were selected based on prior research and experimental tuning. The models were trained using the Adam optimizer, with a learning rate of 0.01 and a batch size of 500. The activation functions used were ReLU for hidden layers and Softmax for the output layer, allowing multiclass classification. The models were trained for 30 epochs, with early stopping to prevent overfitting.

Table 7: Model hyperparameters

Hyper-parameters	Value/Utilizing
Dropout	0.2
Optimizer	Adam

(Continued)

Table 7 (continued)

Hyper-parameters	Value/Utilizing
Kernal size	3 × 3
Pooling size	2 × 2
Learning rate	0.01
Epochs	30
Activation function	ReLU and Softmax
Batch size	500
Verbose	1
Bias	Zeros
Weight	Glorot_uniform

3.4 Model Evaluation

We evaluated each model's performance using accuracy, precision, recall, F1 score, and Area Under the Curve (AUC). We calculated these metrics for melanoma and non-pigmented lesion classification, ensuring consistency across evaluations.

4 Results

4.1 Dataset

We evaluate performance by using the freely available 2019 ISIC challenge dataset. The dataset consists of 25,331 images, divided into two sections. The first portion comprised 80%, or 20,265 images, of the training dataset, while the second comprised 20%, or 5066 images, for testing purposes. We evaluated each classifier on the original image test set to determine the model's efficacy. The images illustrate many types of skin cancer, including melanoma, basal cell carcinoma, benign keratosis, dermatofibroma, actinic keratosis, and pigmented nevus. Table 8 comprehensively summarises the number of photos in each category.

Table 8: Distribution of images of the classes of melanoma and non-melanoma cells

Skin lesion	Training set	Testing set	Total
Melanoma cell	4525	862	5387
Nevus	12,769	2498	15,267
Seborrheic keratosis	2634	519	3153
Basal cell carcinoma	3318	596	3914
Actinic keratosis	873	178	1051
Dermatofibrosarcoma	245	49	294
Vascular lesion	262	54	316
Squamous cell carcinoma	628	159	787
Total	25,254	4915	30,169

4.2 Evaluation

While it is desirable to have high classification performance across all classes, accurately predicting all skin cancers, particularly those with a high mortality rate, such as melanoma, takes precedence over incorrectly predicting a benign lesion.

We assess the effectiveness of the DL-based classification strategy using proposed classification algorithms. We evaluate the efficacy of the DL models in categorizing pigmented and non-pigmented skin lesions. We perform this examination at the beginning of the operation. Later on, the approach achieved a high success rate in the classification, as shown in Table 9.

Table 9: Pigmented and non-pigmented categorization

Method	Acc.	Sen.	Spe.	Precision
LSTM	0.9491	0.9411	0.9385	0.9473
VGG19	0.8926	0.8821	0.8910	0.8951
ResNet50	0.9264	0.9190	0.9210	0.9218
AlexNet	0.8882	0.8877	0.8920	0.8865

The next phase involves examining deep-learning models to classify skin lesions as melanoma or pigmented nevus. Finally, we assess the ability of the third DL model to classify non-pigmented malignant and benign skin disorders. This evaluation confirms the effectiveness of the recommended models.

4.3 Experiment Results: Pigmented vs. Non-Pigmented Classes

Table 9 summarises the results of categorizing pigmented cancers and benign classes. This table displays the count of classes and test photos used to evaluate the performance of the classification. Table 9 also displays the overall results of the categorization process.

4.4 Experimental Results: Pigmented Tumor vs. Benign Classes

Table 10 summarises the classification findings of pigmented tumours and benign classes by displaying the number of photos used for training and testing assessment results. This table also presents the overall classification results.

Table 10: Pigmented tumour and benign classes

Method	Acc.	Sen.	Spe.	Precision
LSTM	0.9531	0.9502	0.9462	0.9510
VGG19	0.9055	0.9020	0.8988	0.9042
ResNet50	0.9178	0.8990	0.9010	0.9018
AlexNet	0.9170	0.9212	0.920	0.9232

4.5 Experiment Results: Melanoma vs. Pigmented Nevus Classes

A summary of the findings from the categorization of pigmented nevus and melanoma can be seen in Table 11, which also contains the findings from the performance assessment.

Table 11: Melanoma and pigmented nevus classes

Method	Acc.	Sen.	Spe.	Precision
LSTM	0.9490	0.9431	0.9396	0.9480
VGG19	0.9035	0.8966	0.8907	0.9025
ResNet50	0.9130	0.910	0.9065	0.9118
AlexNet	0.8932	0.8902	0.8874	0.8916

5 Discussion

Three experiments were conducted. 1. Classification of pigmented and non-pigmented classes. 2. Classification of pigmented tumours and benign classes. 3. Classification of melanoma and pigmented nevus classes.

The information in Tables 9–11 shows that the complementing LSTM model did better than the other three models in the three classification tests we did on the ISIC 2019 dataset in terms of accuracy, sensitivity, and specificity. Table 12 also shows the comparison between our results and some previous related studies, which displays the superiority of our proposed networks over the rest of the networks.

Table 12: Compares the performance of our proposed networks with the comparative algorithms in ISIC-17, ISIC-18, and ISIC-19 in terms of accuracy, precision, sensitivity, specificity, and F1 score

Method	Acc.	Sen.	Spe.	Precision
[9]	0.9325	0.9325	0.9064	0.9397
[36]	0.8963	0.8993	0.9215	0.9129
[37]	0.865	0.556	0.785	–
[38]	0.877	0.8726	0.8218	–
[39]	0.8315	0.83	–	0.89
Our study	0.9531	0.9502	0.9462	0.9510

The graphs illustrate the training results of the proposed models for distinguishing melanoma and pigmented cells, non-melanoma cells, tumour cells, and benign cells. Figs. 5–7 display these graphs.

Metadata, which includes sociodemographic information about patients, is needed to prove that imbalance or under-representation biases exist [40]. The most direct route to resolving this issue is, where feasible, to augment the dataset with photos and information from patients belonging to under-represented groups. Another option is to do further validation, such as prospective studies, to ensure the model's resilience.

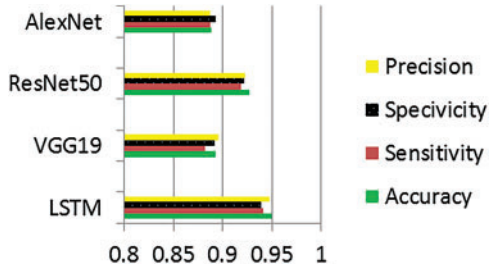

Figure 5: Performance evaluation of pigmented and non-pigmented classes

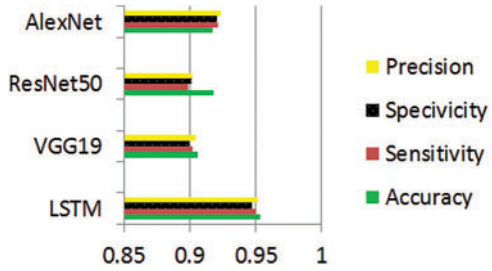

Figure 6: Performance evaluation of pigmented tumor and benign classes

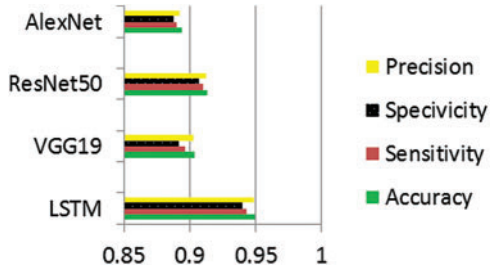

Figure 7: Performance evaluation of melanoma and pigmented nevus classes

An intriguing conversation about the makeup of the training dataset emerged during [41]. The training dataset's limitations in the clinical presentation spectrum, variability in picture collection settings, and limited clinical information raised concerns about the generality of automated diagnosis. These issues pertained to the fact that the training dataset had constraints. A common and often inherent issue with healthcare data is the under-representation of clinical or demographic categories, which may limit the model's potential for generalisation.

Clinically, close-up photographs can effectively aid in the artificial categorisation of skin lesions. The first step that a doctor takes in determining whether or not to continue with dermoscopy is to perform a macroscopic evaluation of a lesion. It is possible that clinical photographs of the lesion can offer extra information that is not evident by dermoscopy. These additional data include the pearly look and shining surface of seborrhoeic keratosis, as well as the "stuck-on" aspect of the condition [42]. Smartphone apps could potentially use these datasets of clinical photographs to train their algorithms. However, even the most advanced of these algorithms still have a significant distance to go.

Shimizu et al. [6] introduced VGG19, a 19-layer convolutional neural network, as an approach for picture classification. The structure consists of three fully interconnected layers and sixteen

convolutional layers. We dedicate the first three convolutional layers to classification and use the remaining sixteen layers for feature extraction.

He et al. [43] introduced ResNet, an enhanced CNN iteration that uses residual blocks. We designed this architecture to tackle the issue of gradient degradation in very deep networks. In these networks, the accuracy first reaches a saturation point. However, it then quickly deteriorates owing to a drop in gradient values.

AlexNet, an efficient, simple CNN Alex Krizhevsky et al. suggested the idea at the 2012 ImageNet Large Scale Visual Recognition Challenge (ILSVRC-2012) [44]. The architecture consists of convolutional, pooling, ReLU, and connected layers. Three layers make up AlexNet's five convolutional layers: a pooling layer, an initial layer, an intermediate layer, and a final layer.

6 Conclusions

We have introduced a DL-based classification technique for skin lesions. It employs four forms of DL. We can classify skin lesions using the provided models as pigmented or non-pigmented. This classification enables the identification of types such as basal cell carcinoma and squamous cell carcinoma. The evaluation data indicates that the LSTM DL model achieves accuracy and sensitivity values. Furthermore, it demonstrates that the melanoma and pigmented nevus classes exhibit classification abilities compared to models.

Based on these results, using the other three models, it seems harder to tell the difference between skin lesions in the Melanoma and non-category than between Melanoma and pigmented nevus. This difficulty arises because both groups encompass a range of skin abnormalities. Additionally, each of these four models uses several training photographs. Moreover, we have determined that identifying a non-pigmented tumour skin lesion is more difficult than identifying a pigmented skin lesion. Moreover, our findings indicate that the LSTM model had greater effectiveness in this aspect than the other models used.

Limitations of the Method Used: The study's models may not generalize well due to a limited and potentially biased dataset that doesn't represent diverse skin types.

Shortcomings of This Method: The computational complexity and need for extensive labelled data can hinder real-time clinical application and widespread implementation.

Prospects for the Future: Future efforts should focus on diversifying datasets, integrating multimodal data for improved accuracy, and developing lightweight models for mobile use to enhance accessibility in dermatological care.

Acknowledgement: The authors express gratitude to the medical staff and nurses at Nasiriyah General Hospital and Turkish Hospital in Nasiriyah City for their essential support and insight into the research. I appreciate AL-Ayen University's assistance with this research.

Funding Statement: The authors received no specific funding for this study.

Author Contributions: Conceptualization, Rafid Sagban; Methodology, Rafid Sagban; Software, Rafid Sagban; Validation, Saadaldeen Rashid Ahmed; Formal analysis and writing—original draft preparation, Haydar Abdulameer Marhoon; Writing—original draft preparation, Rafid Sagban. All authors reviewed the results and approved the final version of the manuscript.

Availability of Data and Materials: The data can be accessed through the Kaggle website as it is open source from the following link: https://www.kaggle.com/datasets/andrewmvd/isic-2019 (accessed on 09 December 2024).

Ethics Approval: Not applicable.

Conflicts of Interest: The authors declare no conflicts of interest to report regarding the present study.

References

[1] N. C. Codella *et al.*, "Skin lesion analysis toward melanoma detection: A challenge at the 2017 International Symposium on Biomedical Imaging (ISBI), hosted by the International Skin Imaging Collaboration (ISIC)," in *2018 IEEE 15th Int. Symp. Biomed. Imaging (ISBI 2018)*, Apr. 2018, pp. 168–172. doi: 10.1109/ISBI.2018.8363547.

[2] M. E. Celebi, N. Codella, and A. Halpern, "Dermoscopy image analysis: Overview and future directions," *IEEE J. Biomed. Health Inform.*, vol. 23, no. 2, pp. 474–478, Mar. 2019. doi: 10.1109/JBHI.2019.2895803.

[3] A. Yilmaz, G. Gencoglan, R. Varol, A. A. Demircali, M. Keshavarz and H. Uvet, "MobileSkin: Classification of skin lesion images acquired using mobile phone-attached hand-held dermoscopes," *J. Clin. Med.*, vol. 11, no. 17, 2022, Art. no. 5102. doi: 10.3390/jcm11175102.

[4] Y. Yuan, M. Chao, and Y. -C. Lo, "Automatic skin lesion segmentation using deep fully convolutional networks with jaccard distance," *IEEE Trans. Med. Imaging*, vol. 36, no. 9, pp. 1876–1886, Sep. 2017. doi: 10.1109/TMI.2017.2695227.

[5] J. Dinnes *et al.*, "Dermoscopy, with and without visual inspection, for diagnosing melanoma in adults," *Cochrane Database Syst. Rev.*, vol. 12, no. 12, 2018, Art. no. CD011902. doi: 10.1002/14651858.CD011902.pub2.

[6] K. Shimizu, H. Iyatomi, M. E. Celebi, K. -A. Norton, and M. Tanaka, "Four-class classification of skin lesions with task decomposition strategy," *IEEE Trans. Biomed. Eng.*, vol. 62, no. 1, pp. 274–283, Jan. 2015. doi: 10.1109/TBME.2014.2348323.

[7] S. Abdelouahed, Y. Filali, and A. Aarab, "An improved segmentation approach for skin lesion classification," *Stat. Optimiz. Inform. Comput.*, vol. 7, no. 2, pp. 456–467, May 2019. doi: 10.19139/soic.v7i2.533.

[8] C. Barata, M. E. Celebi, and J. S. Marques, "Explainable skin lesion diagnosis using taxonomies," *Pattern Recognit.*, vol. 110, Feb. 2021, Art. no. 107413. doi: 10.1016/j.patcog.2020.107413.

[9] I. Iqbal, M. Younus, K. Walayat, M. U. Kakar, and J. Ma, "Automated multiclass classification of skin lesions through deep convolutional neural network with dermoscopic images," *Comput. Med. Imaging Graph.*, vol. 88, 2021, Art. no. 101843. doi: 10.1016/j.compmedimag.2020.101843.

[10] Y. Peng, N. Wang, Y. Wang, and M. Wang, "Segmentation of dermoscopy image using adversarial networks," *Multimed. Tools Appl.*, vol. 78, no. 8, pp. 10965–10981, Sep. 2018. doi: 10.1007/s11042-018-6523-2.

[11] E. Pérez and S. Ventura, "An ensemble-based convolutional neural network model powered by a genetic algorithm for melanoma diagnosis," *Neural Comput. Appl.*, vol. 34, no. 13, pp. 10429–10448, Nov. 2021. doi: 10.1007/s00521-021-06655-7.

[12] A. Ameri, "A deep learning approach to skin cancer detection in dermoscopy images," *J. Biomed. Phys. Eng.*, vol. 10, no. 6, pp. 801–806, Dec. 2020. doi: 10.31661/jbpe.v0i0.2004-1107.

[13] S. S. Han, M. S. Kim, W. Lim, G. H. Park, I. Park and S. E. Chang, "Classification of the clinical images for benign and malignant cutaneous tumors using a deep learning algorithm," *J. Investig. Dermatol.*, vol. 138, no. 7, pp. 1529–1538, Jul. 2018. doi: 10.1016/j.jid.2018.01.028.

[14] M. Shafiq and Z. Gu, "Deep residual learning for image recognition: A survey," *Appl. Sci.*, vol. 12, no. 18, Sep. 2022, Art. no. 8972. doi: 10.3390/app12188972.

[15] Z. Ma and J. M. R. S. Tavares, "Effective features to classify skin lesions in dermoscopic images," *Expert. Syst. Appl.*, vol. 84, pp. 92–101, Oct. 2017. doi: 10.1016/j.eswa.2017.05.003.

[16] A. A. Adegun and S. Viriri, "Deep learning-based system for automatic melanoma detection," *IEEE Access*, vol. 8, pp. 7160–7172, 2020. doi: 10.1109/ACCESS.2019.2962812.
[17] J. A. A. Salido and C. Ruiz Jr, "Using deep learning for melanoma detection in dermoscopy images," *Int. J. Mach. Learn. Comput.*, vol. 8, no. 1, pp. 61–68, Feb. 2018. doi: 10.18178/ijmlc.2018.8.1.664.
[18] I. Iqbal, K. Walayat, M. U. Kakar, and J. Ma, "Automated identification of human gastrointestinal tract abnormalities based on deep convolutional neural network with endoscopic images," *Intell. Syst. Appl.*, vol. 16, Nov. 1, 2022, Art. no. 200149. doi: 10.1016/j.iswa.2022.200149.
[19] E. Göçeri, "Impact of deep learning and smartphone technologies in dermatology: Automated diagnosis," in *2020 Tenth Int. Conf. Image Process. Theory Tools Appl. (IPTA)*, Nov. 2020, pp. 1–6. doi: 10.1109/IPTA50016.2020.9286651.
[20] Y. Liu *et al.*, "A deep learning system for differential diagnosis of skin diseases," *Nat. Med.*, vol. 26, no. 6, pp. 900–908, Jun. 2020. doi: 10.1038/s41591-020-0842-3.
[21] L. R. Soenksen *et al.*, "Using deep learning for dermatologist-level detection of suspicious pigmented skin lesions from wide-field images," *Sci. Transl. Med.*, vol. 13, no. 581, Apr. 2021, Art. no. eabb3652. doi: 10.1126/scitranslmed.abb3652.
[22] A. Rezvantalab, H. Safigholi, and S. Karimijeshni, "Dermatologist-level dermoscopy skin cancer classification using different deep learning convolutional neural networks algorithms," 2018, doi: 10.48550/arXiv.1810.10348.
[23] M. M. Musthafa, T. R. Mahesh, V. Vinoth Kumar, and S. Guluwadi, "Enhanced skin cancer diagnosis using optimized CNN architecture and checkpoints for automated dermatological lesion classification," *BMC Med. Imaging*, vol. 24, no. 1, 2024, Art. no. 201. doi: 10.1186/s12880-024-01356-8.
[24] S. G. Malik, S. S. Jamil, A. Aziz, S. Ullah, I. Ullah and M. Abohashrh, "High-precision skin disease diagnosis through deep learning on dermoscopic images," *Bioengineering*, vol. 11, no. 9, 2024, Art. no. 867. doi: 10.3390/bioengineering11090867.
[25] H. Guan *et al.*, "Dermoscopy-based radiomics help distinguish basal cell carcinoma and actinic keratosis: A large-scale real-world study based on a 207-combination machine learning computational framework," *J. Cancer*, vol. 15, no. 11, 2024, Art. no. 3350. doi: 10.7150/jca.94759.
[26] I. Matas, C. Serrano, F. Silva, A. Serrano, T. Toledo-Pastrana and B. Acha, "AI-driven skin cancer diagnosis: Grad-CAM and expert annotations for enhanced interpretability," 2024, *arXiv:2407.00104*.
[27] M. M. Saraiva *et al.*, "Deep learning and high-resolution anoscopy: Development of an interoperable algorithm for the detection and differentiation of anal squamous cell carcinoma precursors—A multicentric study," *Cancers*, vol. 16, no. 10, 2024, Art. no. 1909. doi: 10.3390/cancers16101909.
[28] G. H. Dagnaw, M. El Mouhtadi, and M. Mustapha, "Skin cancer classification using vision transformers and explainable artificial intelligence," *J. Med. Artif. Intell.*, 2024. doi: 10.21037/jmai.
[29] M. M. Hossain, M. M. Hossain, M. B. Arefin, F. Akhtar, and J. Blake, "Combining state-of-the-art pre-trained deep learning models: A noble approach for skin cancer detection using max voting ensemble," *Diagnostics*, vol. 14, no. 1, 2023, Art. no. 89. doi: 10.3390/diagnostics14010089.
[30] H. Y. Huang, H. T. Nguyen, T. L. Lin, P. Saenprasarn, P. H. Liu and H. C. Wang, "Identification of skin lesions by snapshot hyperspectral imaging," *Cancers*, vol. 16, no. 1, 2024, Art. no. 217. doi: 10.3390/cancers16010217.
[31] W. Yuan, Z. Du, and S. Han, "Semi-supervised skin cancer diagnosis based on self-feedback threshold focal learning," *Discover Oncol.*, vol. 15, no. 1, 2024, Art. no. 180. doi: 10.1007/s12672-024-01043-8.
[32] C. E. A. Tai, E. Janes, C. Czarnecki, and A. Wong, "Double-condensing attention condenser: Leveraging attention in deep learning to detect skin cancer from skin lesion images," 2023, *arXiv:2311.11656*.
[33] A. Mumuni and F. Mumuni, "Data augmentation: A comprehensive survey of modern approaches," *Array*, vol. 16, 2022, Art. no. 100258. doi: 10.1016/j.array.2022.100258.
[34] K. Maharana, S. Mondal, and B. Nemade, "A review: Data pre-processing and data augmentation techniques," *Glob. Transit. Proc.*, vol. 3, no. 1, pp. 91–99, 2022.
[35] K. Alomar, H. I. Aysel, and X. Cai, "Data augmentation in classification and segmentation: A survey and new strategies," *J. Imaging*, vol. 9, no. 2, 2023, Art. no. 46.

[36] M. Michalska-Ciekańska, "Multiclass skin lesions classification based on deep neural networks," *Informatyka, Automatyka, Pomiary w Gospodarce i Ochronie Środowiska*, vol. 12, no. 2, pp. 40–54, 2022. doi: 10.1016/j.compmedimag.2018.05.004.

[37] B. Harangi, "Skin lesion detection based on an ensemble of deep convolutional neural networks," 2017. doi: 10.1016/j.jbi.2018.08.006.

[38] A. Mahbod, G. Schaefer, I. Ellinger, R. Ecker, A. Pitiot and C. Wang, "Fusing fine-tuned deep features for skin lesion classification," *Comput. Med. Imaging Graph*, vol. 71, pp. 19–29, Jan. 2019. doi: 10.1016/j.compmedimag.2018.10.007.

[39] S. S. Chaturvedi, K. Gupta, and P. S. Prasad, "Skin lesion analyzer: An efficient seven-way multiclass skin cancer classification using MobileNet," in *Advanced Machine Learning Technologies and Applications*. Singapore: Springer. 2021, pp. 165–176. doi: 10.1007/978-981-15-3383-9_15.

[40] Z. C. Navarrete-Dechent, S. W. Dusza, K. Liopyris, A. A. Marghoob, A. C. Halpern and M. A. Marchetti, "Automated dermatological diagnosis: Hype or reality?" *J. Investig. Dermatol.*, vol. 138, no. 10, Oct. 2018, Art. no. 2277. doi: 10.1016/j.jid.2018.04.040.

[41] S. S. Han *et al.*, "Deep neural networks show an equivalent and often superior performance to dermatologists in onychomycosis diagnosis: Automatic construction of onychomycosis datasets by region-based convolutional deep neural network," *PLoS One*, vol. 13, no. 1, Jan. 2018, Art. no. e0191493. doi: 10.1371/journal.pone.0191493.

[42] J. Yap, W. Yolland, and P. Tschandl, "Multimodal skin lesion classification using deep learning," *Exp. Dermatol.*, vol. 27, no. 11, pp. 1261–1267, Nov. 2018. doi: 10.1111/exd.13777.

[43] K. He, X. Zhang, S. Ren, and J. Sun, "Deep residual learning for image recognition," in *Proc. IEEE Conf. Comput. Vis. Pattern Recognit.*, 2016, pp. 770–778. doi: 10.1109/CVPR.2016.90.

[44] A. Krizhevsky, I. Sutskever, and G. E. Hinton, "ImageNet classification with deep convolutional neural networks," *Advanc Neural Informat Process Systems*, vol. 25, 2012.